

CRYSTAL CHEMISTRY OF MILARITE

P. ČERNÝ AND F. C. HAWTHORNE

Department of Earth Sciences, University of Manitoba, Winnipeg, Manitoba R3T 2N2

E. JAROSEWICH

Division of Mineralogy, National Museum of Natural History, Smithsonian
Institution, Washington, D.C. 20560, U.S.A.

ABSTRACT

New structure refinements were performed in Mo/C radiation on selected milarite crystals from Kings Mt. and Věžná. The former, a 10.420(2), c 13.810(9) Å, gave $R = 5.4\%$ for all 825 reflections and $R = 4.6\%$ for 538 reflections with $F_o > 3\sigma$. These refinements confirm the restriction of Al and Be to the linking T(2) tetrahedra, and location of "excess" alkalis plus water at the B sites. No deviation from hexagonal symmetry is found; apparently positional disorder (of the B -site species and Ca) parallel to z occurs in crystals with high contents of alkali, Be and H₂O. Milarites display an extensive range of the substitution $\text{Be}^{T(2)} + \text{Na}^B \rightleftharpoons \text{Al}^{T(2)} + \square^B$, with $\text{Be}/(\text{Be} + \text{Al})$ variable from 0.42 to 0.85. Other substitutions are insignificant or doubtful. Molecular H₂O does not appear to be an essential constituent of milarite, being nonstoichiometric relative to any cation and located in a position excluding any possible bonding role. The presence of water affects the cell dimensions of natural milarites, a increasing slightly and c decreasing sharply with increasing H₂O. Samples dehydrated at \sim thirty degrees below the onset of incongruent melting [CaBeSiO₄ + tridymite (+ quartz) + melt] show cell dimensions that correlate with the T(2) population, both a and c decreasing with increasing Be content. No significant correlation of density with composition is apparent, although a crystal's density should increase with the B -site occupancy as do indices of refraction and birefringence. Optical anomalies may be caused by compositional differences among the nonequivalent growth pyramids, mainly in terms of B -site population and H₂O in particular. The consequent slight differences in cell dimensions generate strain, which is enhanced during differential contraction upon cooling after crystallization. The presence or absence of optical anomalies seems to be regulated by nucleation and growth rates rather than by the bulk composition.

Keywords: milarite, crystal-structure analysis, beryllium, cell dimensions, optical anomalies, crystal chemistry.

SOMMAIRE

La structure de la milarite a été à nouveau affinée,

en radiation Mo/C, sur cristaux de Kings Mt. et de Věžná. Celui de Kings Mt., a 10.420(2), c 13.810(9) Å, par exemple, donne un résidu $R = 5.4\%$ pour l'ensemble des 825 réflexions et 4.6% pour les 538 réflexions à $F_o > 3\sigma$. Ces affinements confirment que Al et Be sont confinés aux tétraèdres T(2) et que l'excès d'alcalin, tout comme l'eau, occupe les sites B . On n'observe aucune déviation de l'holoédrie hexagonale; on note, parallèlement à z , un désordre (qui semble être de position) des éléments des sites B et du calcium, dans les cristaux à haute teneur en alcalins, Be et H₂O. La milarite possède un domaine étendu de substitution, $\text{Be}^{T(2)} + \text{Na}^B \rightleftharpoons \text{Al}^{T(2)} + \square^B$, avec rapport $\text{Be}/(\text{Be} + \text{Al})$ variable, allant de 0.42 à 0.85. Toute autre substitution est négligeable ou douteuse. L'eau moléculaire, non-stoechiométrique par rapport aux cations et située dans une position qui lui interdit tout rôle de liaison, ne semble pas être essentielle dans la composition de la milarite. L'eau affecte les dimensions de la maille des cristaux naturels, y produisant un léger accroissement de a et une diminution abrupte de c . Pour les cristaux déshydratés à environ trente degrés sous le point de fusion incongrue [CaBeSiO₄ + tridymite (+ quartz) + bain de fusion], a et c diminuent lorsqu'augmente la teneur en Be des sites T(2). La densité ne semble pas en corrélation avec la composition, tandis que les indices de réfraction et la biréfringence s'accroissent en proportion de la population des sites B . Les anomalies optiques seraient dues à des différences de composition, entre pyramides de croissance non-équivalentes quant à la population des sites B et à la teneur en H₂O. Les faibles différences de maille qui en résultent provoquent des tensions internes, qu'accroissent la contraction différentielle due au refroidissement après cristallisation. L'apparition d'anomalies optiques serait dictée, non par la composition globale, mais plutôt par la vitesse de nucléation et de croissance.

(Traduit par la Rédaction)

Mots-clés: milarite, structure cristalline, beryllium, dimensions de la maille, anomalies optiques, chimie cristalline.

INTRODUCTION

The study of milarite has been marked by

several twists since its beginning. Kenngott (1870) named the mineral after its alleged type locality, Val Milar (Milà), Graubünden, in the Swiss Alps; the type material actually came from the nearby Val Giuf (Giuv) (Kuschel 1877), and Val Milar yielded milarite only much later (Parker 1954).

Originally described as a K,Ca-bearing zeolite, milarite was considered to be identical with levyne. The correct formula was established by Palache (1931), who discovered the presence of substantial Be. Sosedko & Telesheva (1962) commented on the variable Al/Be ratio, apparently not balanced by any other substitution. Chistyakova *et al.* (1964) reported different

alkali contents in nonequivalent growth sectors of single crystals, and showed that heating produced significant changes in unit-cell dimensions. Milarite provides a classic example of anomalous optical behavior: morphologically hexagonal crystals consist of biaxial sectors that either change their orientation and shape or disappear upon heating (Ludwig 1877, Des Cloizeaux 1878, Rinne 1885, 1927). The hexagonal symmetry was confirmed by X-ray diffraction (Gossner & Mussnug 1930). The crystal structure was first described by Belov & Tarkhova (1949, 1951) and Ito *et al.* (1952), and commented on by Pasheva & Tarkhova (1953). Bakakin & Solovyeva (1966), Forbes *et al.* (1972) and

TABLE 1. DATA, SAMPLES, AND SOURCES

Data from literature		
#	Locality	Reference
0	Val Giuf, Switzerland	Gossner & Mussnug (1930)
1	Val Giuf, Switzerland	Palache (1931)
2	Val Giuf, Switzerland	Belov & Tarkhova (1949)
3	Val Giuf, Switzerland	Ito <i>et al.</i> (1952)
4	Piz Ault, Switzerland	de Quervain (Hügi 1956)
5	Val Giuf, Switzerland	Černý (1960)
6	Věžná west, Czechoslovakia	Černý (1960)
7	Kola Peninsula, U.S.S.R.	Sosedko (1960), S. & Telesheva (1962)
8	Tittling, Bavaria, Germany	Tennyson (1960)
9	Rangiertunnel, s. of Göschenen, Switzerland	Graeser & Hager (1961)
10	Věžná east, with epididymite, Czechoslovakia	Černý (1963)
11	Kent, Central Kazakhstan, U.S.S.R.	Chistyakova <i>et al.</i> (1964)
12	Maršikov, Czechoslovakia	Staněk (1964)
13	Central Asia, U.S.S.R.	Ľovcheva <i>et al.</i> (1966)
14	Radkovice, columnar after beryllian cordierite, Czechoslovakia	Černý (1967)
15	Radkovice, fibrous after beryl, Czechoslovakia	Černý (1967)
16	Věžná east, with bavenite, Czechoslovakia	Černý (1968)
17	East Siberia, U.S.S.R.; pink	Novikova (1972)
18	East Siberia, U.S.S.R.; green	Novikova (1972)
19	Rössing, S.W. Africa	v. Knorring (1973)
New data		
#	Locality	Source
20	Val Giuf, Switzerland	Roy. Ont. Mus. Ferrier Coll., M4958
21	Val Giuf, Switzerland	Nat. Mus. Nat. Hist. Washington, R11483
22	Val Giuf, Switzerland	Dept. Mineralogy, Univ. J.E. Purkyně Brno, 2036
23	Val Giuf, Graubünden, Switzerland	Nat. Mus. Nat. Hist. Washington, 47014
24	Gwüest, Göschenenalp, Switzerland	research coll. Dr. Th. Hügi, Bern, SA23
25	Guanajuato, Mexico	Nat. Mus. Nat. Hist. Washington, 121230 and 120408
26	Guanajuato, Mexico	Roy. Ont. Museum, 28150
27	Věžná west, Czechoslovakia	Dept. Earth Sci., U. of Manitoba, M3520
28	Věžná west, columnar, Czechoslovakia	research coll. P. Černý
29	Věžná west, radial fibrous, Czechoslovakia	research coll. P. Černý
30	Rössing, Swakopmund, S.W. Africa	Nat. Mus. Nat. Hist. Washington, C6562
31	Foot Mineral Co. spodumene mine, near Kings Mt., N. Carolina	Nat. Mus. Nat. Hist. Washington, 121805
32	Moat Mt., North Conway, N. Hampshire	Nat. Mus. Nat. Hist. Washington
33	Tittling, Bavaria, Germany	research coll. Dr. Chr. Tennyson, Berlin
34	Nedre Lapplagret, Drag near Tysfjord, Norway	coll. R. Kristiansen, Torp, Norway
35	East Siberia, U.S.S.R.; pink	research coll., P. Černý

Bakakin *et al.* (1975) proposed site populations that explained the dehydration-induced changes in the structure.

Černý (1960) described a variety of milarite with uniaxial optics and significant deviations from the generally quoted values of other

TABLE 2. CHEMICAL COMPOSITION AND PHYSICAL PROPERTIES OF MILARITE

#	13	7	17	4	25	31.	1
Locality	Central Asia	Kola	East Sib., pink Piz Ault		Guanajuato ⁱ	Kings Mt. ⁱ	Val Giuf
SiO ₂	63.83	71.12	71.23	70.81	71.35	71.25	71.66
Al ₂ O ₃	13.04	7.70	7.02	4.34	5.68	4.72	4.68
Fe ₂ O ₃	-	-	.12	1.53	-	-	-
B ₂ O ₃	-	-	-	-	-	-	-
BeO	4.68	3.57	4.52	4.25	4.58	5.26	5.24
FeO	-	-	-	-	-	-	-
MnO	-	-	tr.	-	.25	<.01	-
CaO	11.12 ^a	11.55	9.32	11.42	11.40	11.57	11.70
Na ₂ O	.86	.30	1.90	1.17	.17	.19	.46
K ₂ O	4.62	4.80	4.03	5.34	4.95	4.68	4.91
H ₂ O-	-	.14	-	-	.11	.15	-
H ₂ O+	1.38	1.25	1.65	1.20	1.20	1.66	1.07
Total	99.70 ^b	100.43	99.81 ^e	100.06	99.69	99.48	99.72
Si	T(1) ₂₄	21.51	23.69	23.71	23.87	23.85	23.85
Al	T(2) ₆	5.19	3.02	2.75	1.72	2.24	1.83
Fe		-	-	.03	.39	-	-
B		-	-	-	-	-	-
Be		3.79	2.86	3.61	3.44	3.68	4.19
ΣT(2)		8.98 [?]	5.88	6.39	5.55	5.92	6.02
ΣT(1) + T(2)		30.49	29.57	30.10	29.42	29.77	29.87
Be/(Be + Al)		.42	.49	.56	.62	.62	.70
Ca ₂₊	A ₄	3.97 ^c	4.00	3.32	4.00	4.00	4.00
Fe		-	-	-	-	-	-
Mn		-	-	-	-	-	-
K	C ₂	1.98	2.00	1.71	2.00	2.00	2.00
Na		.02	-	.29	-	-	-
Na	B ₄	.54	.19	.93	.77	.11	.30
K		-	.04	-	.29	.11	.09
Ca		-	.12	-	.12	.08	.17
H ₂ O		1.55	1.39	1.84	1.35	1.33	1.18
ΣB-site valences		.54 ⁺	.47 ⁺	.93 ⁺	1.32 ⁺	.38 ⁺	.73 ⁺
ΣB-site occupancy		2.09	1.74	2.77	2.53	1.63	1.74
D meas.		2.56	-	2.51	2.551	2.547	2.557 ⁹
D calc.		2.605 ^d	2.597 ^d	2.57	-	2.560	2.547
n _e		-	1.537	1.533	-	-	1.537
n _w		-	1.538	1.536	-	-	1.5385
n _w meas.		1.534 ^d	-	-	-	1.535	-
n _m calc. (m) ^k		1.538 ^d	-	1.530	1.541	1.530	1.538
n _m calc. (c) ^l		1.547 ^d	1.547 ^d	1.542	-	1.539	1.536
optical symmetry		patchy extinction	sector-zoning	wavy extinction	?	wavy to moiré	sector-zoning
a/c	natural	10.392(3)	10.40	10.397(9)	-	10.408(2)	10.412(4)
c/a		13.758(5)	13.70	13.770(5)	-	13.826(6)	13.785(9)
V/a		1.324	1.317	1.324	-	1.327	1.324
		1286.7 ^d	1283.2 ^d	1289.0 ^d	-	1297.1	1294.2
							1294.5
a/c	heated	10.395(3)	-	10.379(9)	-	10.373(2)	10.370(2)
c/a		13.829(5)	-	13.820(5)	-	13.874(6)	13.851(4)
V/a		1.331	-	1.331	-	1.337	1.336
		1294.1 ^d	-	1289.2 ^d	-	1292.8	1289.9
							1291.7

a - includes 0.21 SrO

b - includes 0.31 F and oxygen adjustment

c - includes 0.04 Sr

d - our calculation

e - includes 0.02 TiO₂

f - Iovcheva *et al.* (1966) quote a 10.400(3), c 13.743(5), c/a 1.321^d, V 1287.2^d for a sample obtained from Chistyakova

physical constants. Similar milarites have since been described from other localities (Černý 1963, 1967, 1968, Oftedal & Saebö 1965, Raade

1966), but no compositional data have been published for this variety. The physical properties listed by Hügi & Röwe (1970) suggest

TABLE 2, Continued

#	30	11	33	19	18	27	29
Locality	Rössing ⁱ	Kent	Tittling ⁱ	Rössing	East Sib. green	Věžná ^j	Věžná ^j
SiO ₂	71.81	72.43	70.65	72.17	70.76	70.90	71.60
Al ₂ O ₃	3.40	3.85	4.34	3.37	2.91	2.65	2.25
Fe ₂ O ₃	-	.13	-	-	.09	-	-
B ₂ O ₃	.48	-	-	-	-	-	-
BeO	5.07	5.85	6.71	5.87	5.93	6.00	6.30
FeO	-	-	-	-	.05	-	-
MnO	.15	.47	<.01	.15	.07	-	-
CaO	11.60	11.15	10.80	11.20	11.34	11.35	11.20
Na ₂ O	.49	.17	.52	.51	.22	.35	.75
K ₂ O	4.52	4.65	4.97	5.19	5.58	6.30	5.45
H ₂ O-	-	.18	.15	.02	-	-	-
H ₂ O+	1.68	1.43	1.29	1.38	2.40	2.00	2.00
Total	99.20	100.31	99.43	99.86	99.35	99.55	99.55
Si } T(1) ₂₄	24.05	23.90	23.51	24.01	23.98	23.98	24.07
Al ₃₊ } T(2) ₆	1.34	1.50	1.70	1.32	1.16	1.06	.89
Fe ₃₊ } T(2) ₆	-	.03	-	-	.02	-	-
B } T(2) ₆	.27	-	-	-	-	-	-
Be } T(2) ₆	4.09	4.65	5.35	4.69	4.83	4.88	5.08
ΣT(2)	5.70	6.18	7.05	6.01	6.01	5.94	5.97
ΣT(1) + T(2)	29.75	30.08	30.56	30.02	29.99	29.92	30.04
Be/(Be + Al)	.72	.75	.76	.78	.80	.82	.85
Ca ₂₊ } A ₄	3.96	3.87	3.85	3.96	3.97	4.00	4.00
Fe ₂₊ } A ₄	-	-	-	-	.01	-	-
Mn } A ₄	.04	.13	-	.04	.02	-	-
K } C ₂	1.94	1.96	2.00	2.00	2.00	2.00	2.00
Na } C ₂	.06	.04	-	-	-	-	-
Na } B ₄	.25	.07	.35	.33	.14	.23	.49
K } B ₄	-	-	.11	.20	.41	.72	.33
Ca } B ₄	.22	.08	-	.03	.14	.11	.03
H ₂ O } B ₄	1.88	1.58	1.43	1.53	2.71	2.26	2.24
ΣB-site valences	.69	.23	.46	.59	.83	1.18	.88
ΣB-site occupancy	2.35	1.73	1.89	2.09	3.40	3.32	3.09
D meas.	2.541	2.51	2.540	-	2.52	-	-
D calc.	2.563	2.565; 2.554 ^d	2.550	-	-	2.606	2.599
n _e	-	-	1.536	-	1.536	1.546	1.552
n _w	-	-	1.537	-	1.541	1.549	1.555
n _m ^w meas.	1.541	1.542	-	-	-	-	-
n _m ^m calc. (m)	1.537	1.531 ^d	1.538	-	1.536	-	-
n _m ^m calc. (c)	1.542	1.540 ^d	1.539	-	-	1.552	1.551
optical symmetry	fine lamellar	sector-zoning & moiré	sector-zoning & moiré	?	wavy extinction	uniaxial	uniaxial
a } natural	10.409(3) ^h	10.395(1) ^f	10.396(2)	-	-	10.422(3)	10.414(
c } natural	13.791(7)	13.815(5)	13.806(5)	-	-	13.706(7)	13.673(
c/a } natural	1.327	1.329 ^d	1.328	-	-	1.315	1.313
V } natural	1294.0	1292.8 ^d	1292.2	-	-	1289.2	1284.2
a } heated	10.361(2) ^h	-	10.359(3)	-	-	10.334(2)	10.321(
c } heated	13.844(6)	-	13.856(7)	-	-	13.824(6)	13.814(
c/a } heated	1.336	-	1.338	-	-	1.338	1.338
V } heated	1287.0	-	1287.6	-	-	1278.51	1274.3

- g - physical properties and unit-cell dimensions as determined in this study on sample (20)
h - values representative of the analysed material; the bulk of the sample used for heating experiments and shown in Figure 9 under (30a) gave $\underline{a} = 10.401(3)$, $\underline{c} = 13.780(8)$ in natural state.
j - analyst, E. Jarosewich 1971
k - analyst, A.G. Plant 1973; BeO and H₂O by P. Povondra 1967.
l - using measured density
1 - using calculated density

further broadening of the compositional range of milarite, but no adequate extension of compositional variability was detected by electron-microprobe analysis.

Here we present new compositional and X-ray data, and review the chemistry and physical properties of milarite.

EXPERIMENTAL

The study of milarite is complicated by the rarity of its occurrence, compositional variability on a very local scale, anomalous optical properties (possibly associated with chemical heterogeneity) and microscopic inclusions of other species. Consequently, samples from the same locality commonly have different chemical compositions and physical properties.

The samples examined during the present study are listed in Table 1, along with references to the data used from the literature. Numerical symbols of the individual samples and references are used for identification throughout this paper.

New chemical analyses (samples 21, 22, 23, 27) were done using slightly modified microchemical methods of Hillebrand *et al.* (1953). Silica was separated by double evaporation with HCl and volatilized with HF. Aluminum was separated from beryllium with 8-hydroxyquinoline in solution buffered by ammonium acetate. Beryllium was then precipitated at pH 9 and determined as oxide. Sodium and potassium were determined by flame photometry and water, by means of the O-H analyzer. Calcium was precipitated as oxalate. A Material Analysis Company model 400 electron microprobe, operated at 20 kV and 0.03 μ A, was used to analyze samples 27 and 29 (Table 2) and to check for zoning in samples 20 and 30. Natural minerals were used as standards, and the data were reduced using the EMPADR VII program of Rucklidge & Gasparrini (1969).

Unit-cell dimensions were refined from CaF_2 -calibrated X-ray powder diffractograms (12 mm *per* $1^\circ 2\theta$). Crystals of Kings Mt. (no. 31) and Věžná (no. 29) milarites were examined by single-crystal-precession photography using Zr-filtered Mo $K\alpha$ radiation. Single-crystal intensity data for samples 31 and 29 were collected on a Syntex P2₁ automatic four-circle diffractometer according to the experimental procedure of Hawthorne & Ferguson (1975). For sample 31, an irregular, equidimensional crystal of mean radius 0.07 mm was used, and a spherical-absorption correction was performed. For sample 29, two data sets were collected. A stubby,

TABLE 3. MISCELLANEOUS DATA PERTINENT TO STRUCTURE REFINEMENTS

	Kings Mt. (31)	Věžná(29)a	Věžná(29)b
$a(\text{\AA})$	10.420(2)	10.428(6)	10.417(5)
$c(\text{\AA})$	13.810(9)	13.675(9)	13.688(7)
$V(\text{\AA}^3)$	1298.6	1287.8	1286.4
Space group	P6/mcc	P6/mcc	P6/mcc
Z	2	2	2
Rad/Mon	Mo/C	Mo/C	Mo/C
No. of $ F_o $	825	848	992
No. of $ F_o > 3\sigma$	538	380	405
Final R (observed)	4.6%	6.6%	9.7%
Final R (all data)	5.4%	10.5%	14.2%
Final R_w (observed)	4.6%	7.2%	10.9%
Final R_w (all data)	5.0%	9.8%	13.4%
$R = \frac{\sum F_o - F_c }{\sum F_o }$ $R_w = \left(\frac{\sum w F_o - F_c ^2}{\sum w F_o^2} \right)^{1/2}, w = 1$			
Temperature factor form: $\exp\left(-\sum_{i=1}^3 \sum_{j=1}^3 h_i h_j \beta_{ij}\right)$			

prismatic crystal ~ 0.13 mm long with ~ 0.05 mm radius yielded the first data set (29a), whereas the second (29b) was collected on a prismatic crystal ~ 0.50 mm long and with ~ 0.02 mm radius; a cylindrical-absorption correction was performed on both. Standard data-reduction procedures resulted in the numbers of reflections indicated in Table 3, which also lists miscellaneous data pertinent to data collection, reduction and refinement.

In heating experiments, the samples were treated in air in an electric furnace with an estimated temperature fluctuation $\sim \pm 10^\circ\text{C}$, and they were water-dip quenched. Indices of refraction were measured in immersion liquids using a Na-light source. Density was determined partly by floating in heavy liquids measured by the Mohr-Westphal balance, partly by using the Berman balance with toluene as the displacement medium.

Internal consistency of the data on 12 of the analyzed specimens listed in Table 2 was tested by comparing the measured and calculated densities. Samples 7, 13 and 17 show discrepancies of 0.045 to 0.06 in densities and 0.008 to 0.013 in indices of refraction. These three samples are plotted in the diagrams but are not used to establish correlations, as the source of the error is difficult to detect.

STRUCTURE REFINEMENTS

In precession photographs, the Kings Mt. (sample 31) and Věžná (29) milarites display hexagonal symmetry and systematic absences consistent with the space group $P6/mcc$ as observed by previous authors. Thus the deviation

from hexagonal symmetry indicated by the optical data for sample 31 is not apparent in the geometry of the reciprocal lattice. It was noted that the "spot size" on the precession photographs of sample 31 is considerably larger than that for sample 29, which shows uniaxial optics. This may be due to incipient deviations from hexagonal symmetry in sample 31; conversely, 31 may have a greater mosaic spread.

Scattering curves for neutral atoms were taken from Cromer & Mann (1968), with anomalous dispersion corrections from Cromer & Liberman (1970). R indices quoted are of the form listed in Table 3 and expressed as percentages. For each structure refinement, the atomic coordinates of milarite (Bakakin *et al.* 1975) were used as input to the least-squares program RFINE (Finger 1969) and the "excess" components of the structure were not considered.

For the Kings Mt. milarite (sample 31), several cycles of full-matrix least-squares refinement, with a gradually increasing number of variables, resulted in convergence at an R index of 7.1%. A series of difference-Fourier maps calculated at this stage showed significant density only at the B sites; however, the density observed at this position was significantly less than that expected from the total excess components indicated by the chemical analysis. Insertion of all excess components in the B position, together with full-matrix refinement of all variables (except the B -site temperature factor, which was fixed at 1.5 \AA^2), resulted in convergence at an R index of 8.2%. Removal of the B -site cations from the refinement reduced the R index to 7.0%. Refinement of the occupancy of the B sites (by H_2O , represented by oxygen) further reduced the R index to 6.1% and resulted in an occupancy factor of 0.158(17). The total reduction in the weighted R index over this sequence of operations was from 8.3 to 6.0%, a highly significant reduction at the 0.005 confidence level (Hamilton 1965). Temperature factors were converted to an anisotropic form as given in Table 3, and full-matrix least-squares refinement of all variables resulted in convergence at an R index of 4.7%. With the H_2O occupancy of the B position fixed, the temperature factor of the B -site scattering species was changed to anisotropic; the following refinement indicated a significant (but not exaggerated) anisotropy. As the anisotropic behavior of the B -site species appeared similar to that of Ca at the A site, the anisotropic temperature-factors of the B -site species were constrained to be equal to those of the A -site Ca in order that the occupancy

of the B sites could be examined without gross correlations between temperature factor and occupancy parameters at that position. This had an added advantage: the anisotropic behavior of the B -site species was accounted for, albeit crudely, by this method. Full-matrix least-squares refinement of all variables resulted in convergence at an R index of 4.6%. It was noted at this stage that the total scattering-power at the B site [0.158(17) oxygen] was approximately equal to that available from the excess cations indicated by the cell content derived from the chemical analysis. Accordingly, the H_2O at the B sites was replaced by the available Na and Ca, with the H_2O occupancy of the B sites considered variable. Subsequent refinement of all variables converged to an R index of 4.6%, and the H_2O occupancy of the B position was 0.034(18). Examination of difference-Fourier maps calculated after the final cycle of refinement showed no significant concentrations of density anywhere in the structure.

For the Věžná milarite (sample 29a), full-matrix least-squares refinement of an isotropic thermal model with no "excess" components resulted in convergence at an R index of 18%. Again, difference-Fourier maps showed that the only significant density occurred at the B position; for this crystal, the observed density corresponded with that expected from the total excess components indicated by the chemical analysis. Inclusion of all excess components at the B position reduced the R index to 11.3%; refinement of the H_2O occupancy of this position produced no significant change in either occupancy or R index. Temperature factors were converted to an anisotropic form, and full-matrix least-squares refinement of all variables resulted in convergence at an R index of 6.7%. The anisotropic thermal refinement was not satisfactory in two respects. The Ca occupying the A sites showed a very anisotropic vibration, with the ellipsoid greatly elongated along the c axis. In addition, the diagonal temperature-factor coefficients of the Be/Al atoms occupying the $T(2)$ site were all within 3σ of zero, and the ellipsoid was nonpositive and definite. Ca and B -site atoms were then considered disordered along the \bar{b} axis, Ca was allowed to vibrate anisotropically, the isotropic temperature-factor of the B -site cation(s) was fixed at 1.5 \AA^2 and the site population of the B -site H_2O was allowed to vary. Full-matrix refinement of all variables resulted in convergence at an R index of 6.6%.

At this stage, we were suspicious that the positional disordering of the Ca and B -site

atoms might be the result of systematic error in the data, perhaps resulting from a poor absorption-correction. Data from another crystal of Věžná milarite, designated sample 29b, were collected. Full-matrix least-squares refinement of all variables for an isotropic thermal model converged to an *R* index of 16%. The temperature factor for the *B*-site atoms was unrealistically large, suggesting that there was too much scattering power at the *B* site. The isotropic temperature-factor of the *B*-site cation was fixed at 1.5 Å², and the site occupancy of H₂O at the *B* position was refined, converging to a value of 0.30(4), as compared with the value of 0.46 indicated by the chemical analysis. Temperature factors (except the

TABLE 4. ATOMIC PARAMETERS FOR MILARITE STRUCTURE REFINEMENTS

Site	Equi-point	x	y	z	B _{equiv.}
Kings Mt. (31) Milarite					
A	4c	1/3	2/3	1/4	1.90(4)A ²
B	4d	1/3	2/3	0	1.91(2)
C	2a	0	0	1/4	1.48(5)
T(1)	24m	0.0819(1)	0.3359(1)	0.11244(7)	0.66(2)
T(2)	6f	0	1/2	1/4	0.35(6)
O(1)	12i	0.0951(5)	0.3828(5)	0	1.46(7)
O(2)	24m	0.1953(3)	0.2758(4)	0.1345(2)	1.37(5)
O(3)	24m	0.1153(3)	0.4722(3)	0.1808(2)	0.90(4)
Věžná (29a) Milarite					
A	8h	1/3	2/3	0.2646(9)	1.3(2)
B	8h	1/3	2/3	0.0225(13)	1.3
C	2a	0	0	1/4	1.6(1)
T(1)	24m	0.0792(3)	0.3349(3)	0.1141(1)	0.93(4)
T(2)	6f	0	1/2	1/4	1.8(3)
O(1)	12i	0.0908(12)	0.3810(11)	0	1.8(2)
O(2)	24m	0.1928(7)	0.2752(8)	0.1347(4)	1.6(1)
O(3)	24m	0.1131(7)	0.4730(7)	0.1807(4)	1.2(1)
Věžná (29b) Milarite					
A	8h	1/3	2/3	0.2644(12)	1.3(3)
B	8h	1/3	2/3	0.0206(22)	1.3
C	2a	0	0	1/4	1.9(2)
T(1)	24m	0.0794(4)	0.3351(5)	0.1144(2)	1.0(5)
T(2)	6f	0	1/2	1/4	2.5(6)
O(1)	12i	0.0936(22)	0.3832(19)	0	2.6(3)
O(2)	24m	0.1908(11)	0.2729(13)	0.1338(5)	1.8(2)
O(3)	24m	0.1136(11)	0.4741(11)	0.1797(5)	1.3(1)

TABLE 5. SITE-POPULATIONS FROM MILARITE REFINEMENTS

		Kings Mt. (31) Milarite	
B	T(2)	0.030 K + 0.038 Na + 0.034(18) H ₂ O 0.705 Be + 0.295 Al	
		Věžná (29a) Milarite	
B	T(2)	0.046 K + 0.060 Na + 0.23(2) H ₂ O 0.85 Be + 0.15 Al	
		Věžná (29b) Milarite	
B	T(2)	0.046 K + 0.060 Na + 0.17(3) H ₂ O 0.85 Be + 0.15 Al	

TABLE 6. SELECTED INTERATOMIC DISTANCES (Å) AND ANGLES (°) IN FOOTE MINE AND VĚŽNÁ MILARITES

	Kings Mt. (31)	Věžná (29)a	Věžná (29)b
A octahedron			
A-0(3)	2.364(3) x6	2.297(7) x3 2.456(8) x3	2.293(11) x3 2.452(11) x3
<A-O>	2.364	2.377	2.373
O(3)-O(3)	3.744(5) x6	3.761(10) x6	3.743(17) x6
O(3)-O(3)	2.615(5) x3	2.575(9) x3	2.582(16) x3
O(3)-O(3)	3.164(5) x3	3.196(11) x3	3.212(17) x3
<O-O>	3.317	3.323	3.320
O(3)-A-0(3)	104.7(1) x6	100.0(3) x3	99.5(5) x3
O(3)-A-0(3)		109.9(3) x3	109.4(4) x3
O(3)-A-0(3)	67.2(1) x3	65.5(3) x3	65.9(4) x3
O(3)-A-0(3)		84.0(1) x3	85.1(4) x2
<O-A-O>	90.1	90.0	90.0
B polyhedron			
B-0(1)	2.754(5) x3	2.799(11) x3	2.768(19) x3
B-0(3)	3.304(3) x6	3.065(13) x3 3.542(15) x3	3.068(22) x3 3.491(24) x3
	3.121	3.135	3.109
C polyhedron			
C-0(2)	3.019(3)x12	2.999(7) x12	2.985(11)x12
D polyhedron			
D-0(2)	3.166(3)x12	3.146(7) x12	3.120(10)x12
T(1) tetrahedron			
T(1)-0(1)	1.615(2)	1.620(3)	1.628(5)
T(1)-0(2)	1.621(3)	1.615(7)	1.610(10)
T(1)-0(2)	1.622(3)	1.617(6)	1.621(9)
T(1)-0(3)	1.593(3)	1.587(6)	1.583(9)
<T(1)-O>	1.613	1.610	1.611
O(1)-0(2)	2.638(4)	2.630(9)	2.620(14)
O(1)-0(2)	2.657(4)	2.638(10)	2.656(15)
O(1)-0(3)	2.639(3)	2.619(6)	2.606(9)
O(2)-0(2)	2.563(3)	2.551(7)	2.526(12)
O(2)-0(3)	2.647(4)	2.658(8)	2.669(13)
O(2)-0(3)	2.651(4)	2.670(9)	2.691(14)
<O-O>	2.633	2.628	2.628
O(1)-T(1)-0(2)	109.3(2)	108.8(4)	108.0(7)
O(1)-T(1)-0(2)	110.3(2)	109.2(5)	109.6(8)
O(1)-T(1)-0(3)	110.7(2)	109.5(4)	108.5(7)
O(2)-T(1)-0(2)	104.4(2)	104.2(5)	102.8(8)
O(2)-T(1)-0(3)	110.9(2)	112.1(4)	113.4(5)
O(2)-T(1)-0(3)	111.0(2)	112.9(4)	114.2(5)
<O-T(1)-O>	109.4	109.5	109.4
T(2) tetrahedron			
T(2)-0(3)	1.672(3) x4	1.643(6) x4	1.649(8) x4
O(3)-0(3)	2.615(5) x2	2.575(10) x2	2.582(15) x2
O(3)-0(3)	2.742(5) x2	2.685(12) x2	2.678(18) x2
O(3)-0(3)	2.829(5) x2	2.786(11) x2	2.811(17) x2
<O-O>	2.729	2.682	2.690
O(3)-T(2)-0(3)	102.9(2) x2	103.2(4) x2	103.1(7) x2
O(3)-T(2)-0(3)	110.2(2) x2	109.6(4) x2	108.6(5) x2
O(3)-T(2)-0(3)	115.6(2) x2	116.0(4) x2	117.0(7) x2
<O-T(2)-O>	109.6	109.6	109.6
Miscellaneous			
		3.31(2)	3.34(3)
		3.53(2)	3.51(3)
A-B	3.456(2)		
		2.91(2)	2.94(4)
		3.93(2)	3.90(4)
A-T(2)	3.011(1)	3.017(3)	3.014(2)

factor of the *B*-site atoms) were changed to an anisotropic form, and full-matrix least-squares refinement of all variables resulted in convergence at an *R* index of 9.9%. The anisotropic temperature-factors of the *A*-site Ca again indicated an ellipsoid of vibration extremely elongated in the *z* direction. With the *A*- and *B*-site cations disordered along the \bar{b} axis and the H₂O occupancy of the *B* sites considered variable, full-matrix refinement of all

variables converged to an *R* index of 9.7%. Both *T*(1) and *O*(1) had $\beta_{33} = 0$ within one standard deviation, and their vibration ellipsoids were nonpositive and definite; thus, neither refinement of Věžná milarite can be considered completely satisfactory. However, attempts to refine both Věžná sets of data (samples 29a and b) in space group *P6cc* did not result in significant improvements in the refinement; the unsatisfactory aspects of the refinements are considered due to the large number of weak reflections in the data sets of the Věžná crystals.

Final atomic parameters are given in Tables 4 and 5; structure-factor tables are available, at a nominal charge, from the Depository of Unpublished Data, CISTI, National Research Council of Canada, Ottawa, Ontario K1A 0S2. Interatomic distances and angles were calculated with the program ERRORS (L.W. Finger, pers. comm.) and are given in Table 6; the anisotropic temperature-factors are given in Table 7.

STRUCTURE AND CHEMISTRY

General

The structure of milarite is illustrated in Figure 1. Hexagonal Si₁₂O₃₀ double rings of silicate tetrahedra are linked by tetrahedrally coordinated *T*(2) cations and octahedrally coordinated *A* cations into a three-dimensional tetrahedral framework. Sandwiched between adjacent *A* octahedra are the *B* sites, each surrounded by nine oxygens; alternating along the tunnels formed by the stacking of the double hexagonal silicate rings are the *C* and *D* sites,

TABLE 7
ANISOTROPIC TEMPERATURE FACTOR COEFFICIENTS FOR MILARITES

	β_{11}	β_{22}	β_{33}	β_{12}	β_{13}	β_{23}
Kings Mt. (31) Milarite						
A	45(1)	45	36(1)	23	0	0
C	44(2)	44	21(2)	22	0	0
T(1)	21(1)	25(1)	7(4)	12(1)	-1(1)	-1(1)
T(2)	13(5)	4(7)	5(2)	22	0	0
O(1)	71(6)	47(5)	8(1)	33(5)	0	0
O(2)	39(3)	62(4)	18(1)	38(3)	-4(2)	-7(2)
O(3)	30(3)	28(3)	11(1)	15(2)	-1(2)	-4(2)
Věžná (29)a Milarite						
A	27(3)	27	30(9)	13	0	0
C	51(6)	51	22(3)	26	0	0
T(1)	33(3)	37(2)	8(1)	19(3)	0(1)	-2(2)
T(2)	27(12)	131(42)	19(7)	66	0	0
O(1)	100(15)	65(12)	4(3)	50(12)	0	0
O(2)	57(8)	67(9)	17(3)	44(8)	-9(4)	-8(5)
O(3)	42(7)	34(7)	14(2)	17(6)	0(4)	-4(4)
Věžná (29)b Milarite						
A	28(12)	28	26(12)	14	0	0
C	72(9)	72	14(4)	36	0	0
T(1)	44(4)	48(4)	0(1)	25(4)	0(2)	-4(3)
T(2)	55(20)	167(78)	18(10)	83	0	0
O(1)	160(29)	104(23)	-4(4)	76(22)	0	0
O(2)	71(13)	108(17)	5(3)	66(13)	-5(6)	-9(6)
O(3)	50(11)	53(11)	8(3)	29(9)	-1(5)	-7(6)

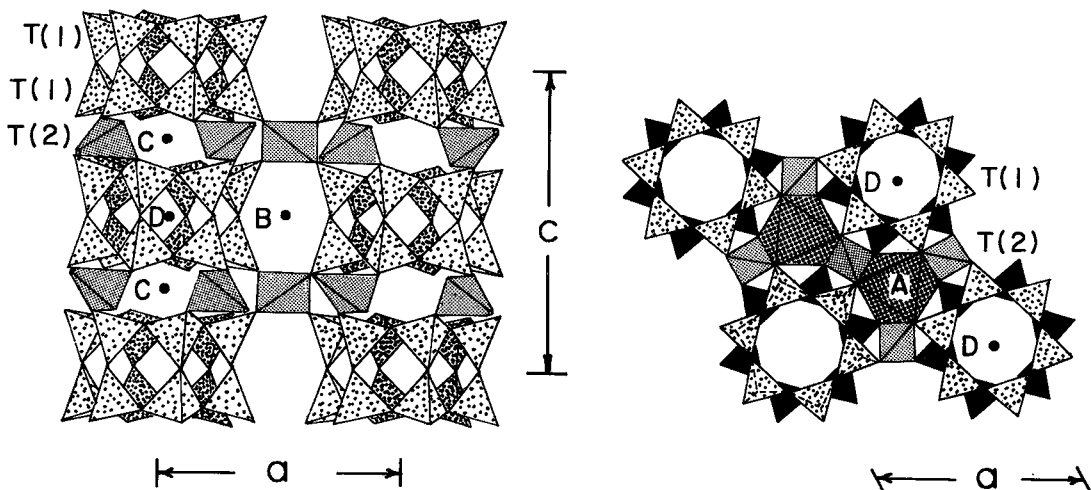


FIG. 1. Crystal structure of milarite viewed parallel to [101] and [001]. Octahedral *A* sites located at the level of the *T*(2) octahedra are omitted in the horizontal projection for clarity.

TABLE 8. CATION AND WATER POSITIONS IN MILARITE

Symbol	Equi-point	C.N.	Site Symmetry	Population
T(1)	24(m)	4	1	Si(Al?)
T(2)	6(f)	4	222	Be, Al(B, Mg, Ti, Zn, Sc)
A	4(c)	6	32	Ca(Mn, Fe, Sr)
B	4(d)	9	6	Na, K, H ₂ O(Ca, H ₃ O?)
C	2(a)	12	62	K(Na, Ba, Y, Yb) ³
D	2(b)	18	6/m	(H ₂ O??)

Modified after Forbes et al. (1972), Table 1.
Elements in parentheses - minor but >0.01 wt.%

each surrounded by twelve and eighteen oxygens, respectively. The general formula for minerals of this structure type may be written (Forbes *et al.* 1972) $A_2^8B_2^9C^{12}D^{18}T(2)_3^4T(1)_{12}^4O_{80}$ with the site populations in milarite given in Table 8, based on the chemical analyses of Table 2 and on the emission-spectrograph analyses of Černý (1960, 1967, 1968), Sosedko & Telesheva (1962), Chistyakova *et al.* (1964), Stanek (1964), Iovcheva *et al.* (1966) and Novikova (1972). These data conform to the idealized average formula of milarite itself, $(K, Na)Ca_2[(Be_2Al)Si_{12}O_{30} \cdot 0.75H_2O]$, as suggested by Palache (1931).

Tetrahedral population and charge balance

Table 2 shows that the Be/(Be + Al) ratio varies between 0.42 and 0.85, the (Be, Al) content (normalized to the ideal total of 6.0) varying correspondingly from $Be_{2.53}Al_{3.47}$ to $Be_{5.10}Al_{0.90}$, as shown in Figure 2. Examination of the T(2)-O bond lengths in the milarite- and tualite-group minerals (Fig. 3) shows that the data of the present study are consistent

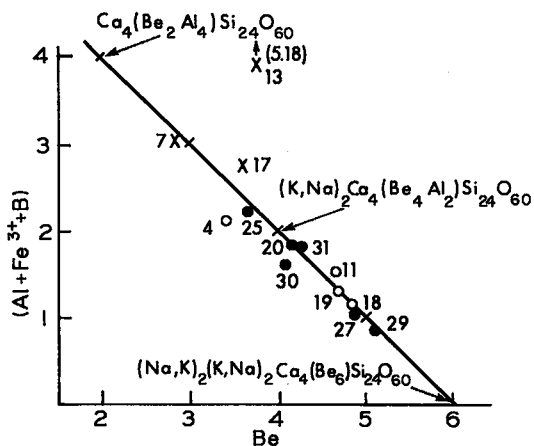


FIG. 2. Plot of Be versus other T(2) cations (Al + Fe³⁺ + B). Most data follow closely the $Be_{e-}(Al + Fe^{3+} + B)_e$ line.

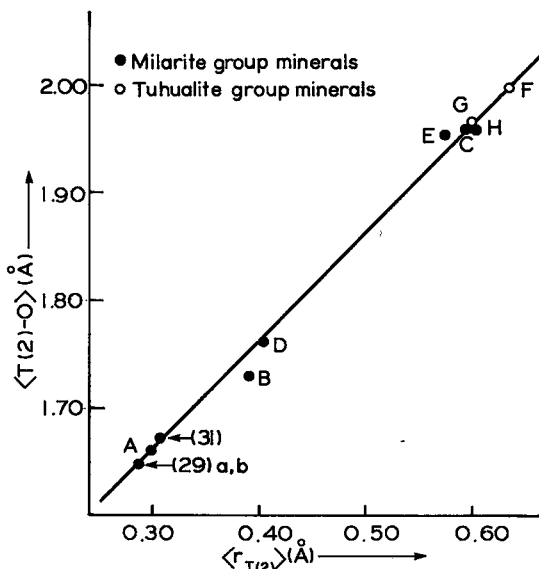


FIG. 3. Plott of the $\langle T(2)-O \rangle$ distances versus $\langle r_{T(2)} \rangle$ for the minerals of the milarite and tualite groups: A milarite, B armenite, C sogdianite (Bakakin *et al.* 1975), D osumilite (Brown & Gibbs 1969), E merrihuete (Khan *et al.* 1971), F tualite (Merlino 1969), G zektzerite (Ghose & Wan 1978), H Zn-milarite (Pushcharovskii *et al.* 1972).

with direct substitution of Be for Al at the T(2) sites. This substitution was noted by Sosedko & Telesheva (1962), but they could not identify the charge-balancing substitution. The obvious way in which electroneutrality

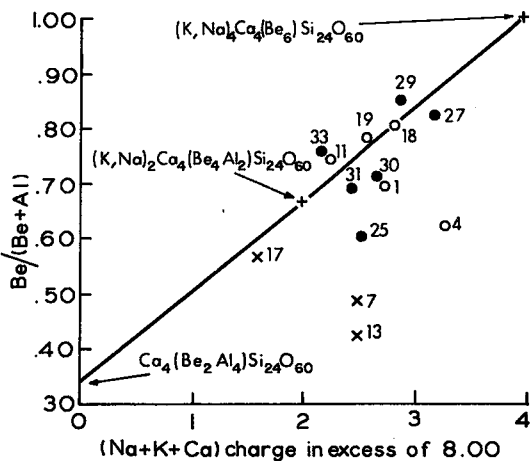


FIG. 4. The Be/(Be + Al) ratio versus the (Na + K + Ca) charge in excess of 8.00, representative of the C- and B-site populations. Solid line indicates the ideal $Be + Na \rightleftharpoons Al$ substitution.

could be maintained on substitution of Be for Al at $T(2)$ is by substitution of alkali metal cations at the B position, which is unoccupied in the ideal formula. This results in the charge-balanced substitution $\text{Be}^{T(2)} + \text{Na}^B \rightleftharpoons \text{Al}^{T(2)} + \square^B$. There seems to be no reason why K could not also participate in this substitution (*cf.*, merrihueite, Khan *et al.* 1971). Similarly, many analyses show a slight excess of Ca that could also occupy the B site. This substitution is examined in Figure 4; the analyses scatter about the ideal relationship, but the correlation is hardly impressive. There is a slight improvement if Ca is not included in the B -site cations, but it is not clear whether this is significant. Although this apparently is the primary substitution, several additional substitutions are possible. However, except for the possible substitution of Ca for K at the C site, they all produce a charge deficiency and cannot help to balance the charge deficiency produced by the $\text{Be} \rightleftharpoons \text{Al}$ substitution. As the K content of the unit cell generally exceeds 2.0 (Table 2), the substitution of "excess" cations into the B position is the only scheme that can balance the charge deficiency produced by the $\text{Be} \rightleftharpoons \text{Al}$ substitution, and hence the coupled substitution indicated above must hold.

Since the substitution of large cations at the B site is the only charge-excess-producing substitution, the data points of Figure 4 should lie along or below the line representing the above substitution, provided there is no error in the chemical analyses. The data tend to scatter more or less randomly about the line (except for certain samples that do lie well below the line); this suggests that in fact additional substitutions are not important and that the scatter about the line represents analytical error. In minerals of this sort, which contain large amounts of high-valence cations and small amounts of low-valence cations, small percentage errors in the analysis of high-valence cations (Si^{4+}) produce a tremendous effect on the assignment of low-valence cations (Na^+ , K^+) to particular positions in the structure where the alkali metal sites are of low multiplicity. In the case of the milarites, the principal coupled-substitution scheme is all but obscured by this effect.

Inspection of analysis 13 (Table 1) shows Si to be significantly less than the ideal value of 24.0, whereas the sum of Al + Be is significantly in excess of 6.0. This suggests the substitution of some Al for Si in $T(1)$; however, electroneutrality is maintained by the sum of $T(1) + T(2)$ cations significantly exceeding 30.0. Thus it is not clear whether this osumilite-

TABLE 9. SCHEMATIC REPRESENTATION OF THE MILARITE SUBSTITUTION SERIES

B_4	C_2	A_4	$T(2)_6$	$T(1)_{24}$	Sample #
H_2O^-		Ca_4	Be_2Al_4	Si_{24}	
H_2O	$(\text{K} > \text{Na})_1$	Ca_4	Be_3Al_3	Si_{24}	—10
H_2O	$(\text{K} > \text{Na})_2$	Ca_4	Be_4Al_2	Si_{24}	—15, 21, 22
$(\text{Na}, \text{K})_1, \text{H}_2\text{O}$	$(\text{K} > \text{Na})_2$	Ca_4	Be_5Al	Si_{24}	—20
$(\text{Na}, \text{K})_2, \text{H}_2\text{O}$	$(\text{K} > \text{Na})_2$	Ca_4	Be_6	Si_{24}	

like population of the tetrahedral double rings is real. Other samples (particularly 7 and 4) that deviate considerably from the ideal substitution line shown on Figure 4 are characterized by $T(2)$ cation sums significantly less than the ideal value of 6.0; whether this reflects analytical error or the presence of additional elements is not clear.

The extent of the main substitution is shown schematically in Table 9. The existence of the Al-free beryllium end-member appears feasible, since the B and C sites can accommodate the necessary alkali metals. However, in nature this species is unlikely, because milarite parageneses are always rich in Al. At the other end of the series, the alkali-free compositions are most unlikely natural minerals, although the (Be_2Al_4) composition may occur as a synthetic phase.

Water

Bakakin *et al.* (1975) showed that water occupies the B positions in the general formula given above, although they proposed that it does not occupy the centre of the surrounding anion polyhedron (the $4b$ position), being slightly disordered in the $8h$ position. Our structural results for the Věžná milarite (sample 29) support this result. Forbes *et al.* (1972) suggested that milarite may contain hydronium ions (H_3O^+) rather than water molecules, and further suggested that if this were the case, then the oxygen atom of the hydronium ion would occupy the $8h$ rather than the $4b$ position, as was found by Bakakin *et al.* (1975) and in this study. However, polarized-infrared-absorption spectra of Kings Mt. (sample 31) and Věžná milarites show the presence of nonbonded molecular water only, apparently in the same chemical and structural environment (G.R. Rossman, pers. comm.). This is in accord with the present study, in which water occurring at the B position is beyond the bonding limit of any of the adjacent cations. In the Věžná milarite (sample 29), positional

disorder of both Ca and H₂O at the *A* and *B* positions, respectively, could promote slight bonding between Ca and H₂O if the correct configuration occurred. However, the infrared-absorption data on these crystals appear to negate this possibility. One interesting result of the present study is that the total electron-density found at the *B* sites in Kings Mt. (sample 31) and Věžná (29b) milarites was not in accord with that indicated by the cell contents calculated from the chemical analyses. With regard to the Věžná results (sample 29), the mean bond-lengths suggest the same site-chemistry at the *T*(1), *T*(2), *A* and *C* sites in the structure for both samples 29a and 29b. Thus, the excess alkali cations occupying the *B* sites should be the same in both crystals to ensure overall electrostatic neutrality. Consequently, any change in occupancy of the *B* sites should involve molecular H₂O, as there seem to be no stoichiometric constraints affecting this species. Although the Věžná crystals (29a and b) were taken from the same cluster of crystals, the physical appearance of each differs considerably. The cluster of crystals consisted of a radiating spray of acicular crystals up to 7 mm long. Where attached to the cavity edge, the crystals were fairly thick (~ 0.06 mm), and sample 29a was taken from this region. A small distance from the base, the crystals thinned rapidly and were ~ 0.02 mm thick along most of their length; sample 29b was taken from this region. Thus, the difference in H₂O contents could reflect a change in ambient conditions of formation or growth rates. Our results for Kings Mt. milarite (sample 31) reveal much less H₂O than the amount indicated by the chemical analysis. However, it should be noted that the amount of H₂O indicated by the structure refinement is highly dependent on the alkali content of the *B* position and hence is strongly influenced by small errors in the chemical analysis or by compositional variability in hand specimen. Infrared-absorption results (G.R. Rossman, pers. comm.) show that some Kings Mt. milarites contain substantial amounts of water. These considerations suggest that the H₂O contents of milarites are highly variable, both in hand specimen and possibly even in individual crystals. Water does not seem to be an essential constituent of milarite, by analogy with osumilite (Olsen & Bunch 1970, Goldman & Rossman 1978), which has been shown to be an anhydrous mineral. The fact that milarites generally contain water whereas osumilites do not presumably reflects the different parageneses of these two

minerals. Also pertinent to the highly variable water content, milarite may contain fluid inclusions that contribute nonstructural H₂O to the chemical analysis.

X-RAY POWDER-DIFFRACTION STUDY

Natural specimens

X-ray powder-diffraction data for milarite obtained in this study correspond in general with published values, but they reveal distinct differences in their dependence on chemical composition. Figure 5 and Table 10 present the data for samples 25 and 29, which have widely different Be/(Be + Al) ratios and H₂O contents. The conspicuous difference between the illustrated patterns is principally due to the remarkable increase in the intensities of the 200 and 300 reflections with increasing occupancy of the *B* position.

Figure 6 shows the unit-cell dimensions of natural milarites. As the data obtained by

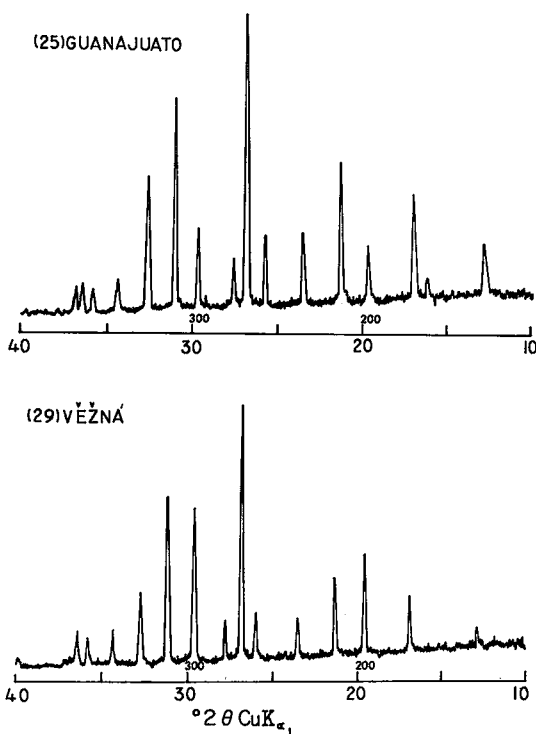


FIG. 5. X-ray powder-diffraction patterns of two milarites representative of the Be- and water-poor (sample 31) and Be- and water-rich (29) varieties. Note the remarkable difference in intensities, attributable mainly to the different H₂O contents.

TABLE 10. X-RAY POWDER DIFFRACTION DATA

MILARITE (25) GUANAJUATO				MILARITE (29) VĚŽNÁ			
1.20 wt.% H ₂ O (1.33 per cell)				2.00 wt.% H ₂ O (2.24 per cell)			
B-site occupancy 1.63				B-site occupancy 3.09			
Be/(Be + Al) = .62				Be/(Be + Al) = .85			
$a = 10.408(2) \text{ \AA}$				$a = 10.414(1) \text{ \AA}$			
$c = 13.826(6) \text{ \AA}$				$c = 13.673(3) \text{ \AA}$			
I_{meas}	$d(\text{\AA})_{\text{meas}}$	$d(\text{\AA})_{\text{calc}}$	hkl	I_{meas}	$d(\text{\AA})_{\text{meas}}$	$d(\text{\AA})_{\text{calc}}$	hkl
16	6.93	6.913	002	6	6.85	6.837	002
7	5.48	5.487	102	-	-	5.448	102
36	5.22	5.209	110	21	5.20	5.207	110
19	4.51	4.511	200	39	4.51	4.509	200
47	4.16	4.160	112	29	4.14	4.142	112
24	3.777	3.778	202	15	3.763	3.764	202
23	3.456	3.457	004	16	3.418	3.418	004
100	3.316	3.311	211	100	3.310	3.307	211
16	3.227	3.228	104	16	3.200	3.206	203
27	3.009	3.007	300	60	3.007	3.006	300
71	2.882	2.880	114	65	2.858	2.858	114
46	2.745	2.744	204	28	2.729	2.730	213
9	2.603	2.604	220	13	2.603	2.603	220
8	2.511	2.519	303	10	2.504	2.509	303
10	2.462	2.502	310	10	2.504	2.501	310
10	2.462	2.462	311	13	2.460	2.460	311
9	2.431	2.437	222	4	2.420	2.433	222
		2.427	214			2.414	214
1	2.265	2.269	304	3	2.255	2.257	304
6	2.198	2.199	313	7	2.193	2.193	313
1	2.149	2.148	215	1	2.132	2.133	215
3	2.107	2.107	116	3	2.090	2.088	116
3	2.045	2.047	321	5	2.044	2.046	321
11	2.026	2.027	314	9	2.019	2.018	314
7	1.967	1.969	410	13	1.967	1.968	410
3	1.950	1.949	411	3	1.945	1.948	411
		1.894	412			1.891	412
12	1.890	1.889	404	8	1.886	1.884	323
		1.888	323			1.882	404
14	1.855	1.855	315	12	1.846	1.846	315

Philips-Norelco diffractometer, scanning $\frac{1}{2}2\theta/\text{min.}$,
Cu K $_{\alpha 1}$ radiation, CaF₂ internal standard ($a = 5.4620 \text{ \AA}$).

different authors on samples from a single locality commonly show considerable scatter, only the new sets of unit-cell dimensions are considered here. Our data, shown in Figure 6 and compared with the compositions listed in Table 2, suggest a distinct trend of a increasing slightly and c decreasing sharply with the general increase in Be/(Be + Al), B-site alkalis and H₂O. The best correlation is with H₂O (Fig. 7); data in the Be/(Be + Al) diagram show considerable scatter (Fig. 8), and the B-site alkalis show little or no correlation.

[Note added in proof: A new set of unit-cell dimensions was obtained by the present authors for the Rössing milarite analyzed chemically by von Knorring (1973: sample 19): a 10.398(4), c 13.812(9) Å. Except in the c versus Be/(Be + Al) plot (Fig. 8), these values follow the established trends between cell dimensions and chemistry.]

Heating experiments

Differential thermal analysis of milarite,

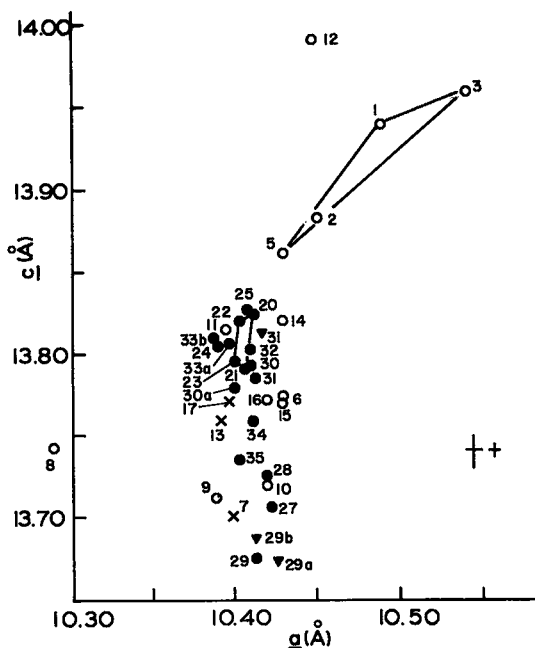


FIG. 6. Unit-cell dimensions of milarite; new data marked by solid dots, data from literature by empty circles and xs. Triangles denote new data obtained by single-crystal methods. Solid lines connect values collected by different techniques, on different samples, of the Val Giuf milarite. Crosses indicate the maximum and minimum single standard errors for the new data.

together with other controlled heating experiments, indicate that significant dehydration starts only above 600°C, and long periods of heating are necessary to expel all the H₂O present. Forbes *et al.* (1972) suggested that the loss of H₂O from the B sites is responsible for the heat-induced changes in the unit-cell dimensions. If true, unit-cell dimensions could be used as a measure of dehydration in heating experiments, and heating to temperatures close to the melting point should lead to (almost) total dehydration, counteracting the influence of H₂O on the unit-cell dimensions.

Temperature-time plots (Fig. 9) show the behavior of milarite (sample 30a) under different heating conditions. The character of the changes in unit-cell dimensions, increasing in magnitude with increasing temperature and leveling off only after prolonged heating, is in accord with the location of H₂O in the B sites. Long runs at high temperatures are evidently necessary to expel the H₂O molecules, which are effectively caged in the [9]-oxygen

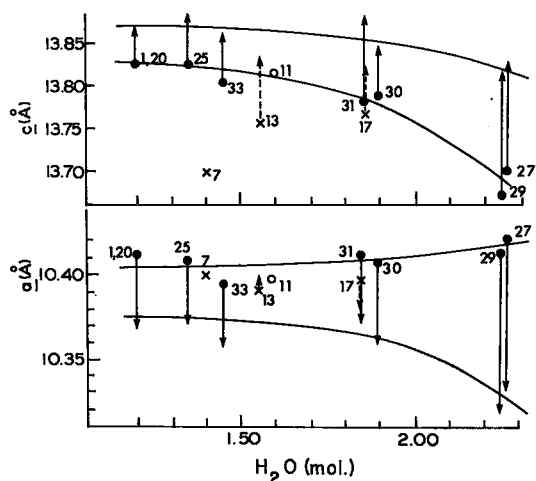


FIG. 7. Variation of the unit-cell dimensions of natural milarite depending on the water content. Symbols as in Figure 6. Unit-cell dimensions after heating at 1050°C for 16 h in air indicated by arrowheads.

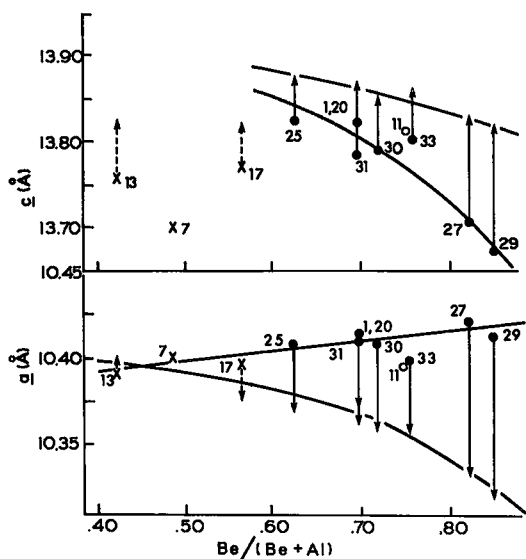


FIG. 8. Variation of the unit-cell dimensions of natural milarites as a function of Be/(Be + Al) ratio; symbols as in Figure 6. Unit-cell dimensions after heating at 1050°C for 16 h in air indicated by arrowheads.

coordination polyhedron surrounding the *B* sites.

Milarite (sample 30a) shows broadening of its X-ray powder-diffraction peaks after short runs at 1070 and 1080°C. Charges treated at 1070°C/72 h show incipient breakdown with formation of CaBeSiO₄ but no indication of

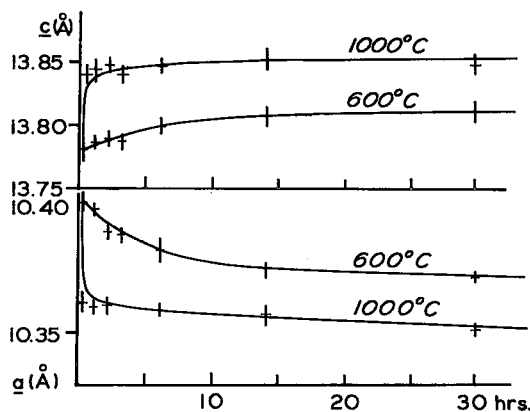


FIG. 9. Changes in unit-cell dimensions of milarite from Rössing (sample 30) with time of heating in air at 600 and 1000°C, after water-dip quenching. Vertical bars indicate a single standard error in the unit-cell dimension.

melting; runs at 1080°C/21 h lead to incongruent melting with formation of CaBeSiO₄, tridymite and possibly some quartz. Complete melting occurs at 1100°C/1 h. Consequently, 1050°C was selected for standard dehydration runs, and a period of 16 hours was considered sufficient, as the interval was well inside the horizontal segment of the temperature–time curves of Figure 9, even at lower temperatures.

Unit-cell dimensions of the heated milarites display extremely poor correlation with the *B*-site alkalis, but the alignment of data against the Be/(Be + Al) ratio is good and much improved over the same correlation for natural hydrous milarites (Fig. 8). This is not altogether unexpected in view of the chemical substitutions discussed above. The substitution of Be for Al in *T*(2) is accompanied by a contraction of the *a* and *c* dimensions, owing to the difference in their ionic radii. The effect of the accompanying introduction of Na into the vacant *B* sites is hard to estimate, as it depends on the relative sizes of the polyhedral cavity either empty or occupied by Na, the values of which are not known. However, it obviously does not cause a substantial expansion of the structure.

The considerable change in unit-cell dimensions upon dehydration, commensurate in magnitude with the original H₂O content, supports the suggestion of Forbes *et al.* (1972) that H₂O does significantly affect the cell dimensions. Since it is present as molecular H₂O, repulsion between H₂O and the surrounding anions presumably prevents the structure from collapsing in the (001) plane when the tem-

perature decreases subsequent to crystallization; thus, dehydration is accompanied by a decrease in a and an increase in c , as is observed (Figs. 7, 8).

PHYSICAL PROPERTIES

The range of measured densities of milarites is very narrow (~ 0.15 g/cm³, excluding one exceptional specimen quoted by Hügi & Röwe 1970), and it is even more restricted for the analyzed specimens listed in Table 2 (~ 0.10 g/cm³). No significant correlation with composition is apparent, except a general tendency to increase with increasing B -site occupancy, as exemplified by the low-density samples 25, 37 and 1, and high-density samples 27 and 29 (Table 2). Increasing H₂O content would compound this effect by reducing the unit-cell volume.

The extremely low birefringence of most milarites makes attempts to measure n_e and n_ω (or n_α and n_γ) impractical; consequently, n_m was either measured directly or calculated. As expected, n_m increases with both B -site occupancy and Be/(Be + Al) ratio, but it shows much better correlation with the former (Fig. 10). The considerable scatter of both measured and calculated n_m is understandable in terms of analytical errors combined with the optical inhomogeneity of sector-zoned crystals. For example, it appears that the low indices of refraction quoted for milarite samples 7 and 13 were measured on fragments totally nonrepresentative of the material used for chemical analysis.

The birefringence of milarite tends to increase with n_m and the B -site occupancy but the trend is poorly developed. The optics of biaxial sectors influence the relation of composition to birefringence much more than to n_m . In general, it can be concluded that the concomitant increase in n_m and birefringence with increasing alkalis and H₂O is analogous to that displayed by beryl (*e.g.*, Beus 1960, Feklitchev 1964, Černý & Hawthorne 1976).

The extremely low indices of refraction of several Swiss milarites given by Hügi & Röwe (1970), 1.512 to 1.524, invite comment because they lie below the range of indices measured for the chemically analyzed specimens (Table 2). An extension of the substitutional series shown in Table 9 towards alkali-free Al-enriched members, which would decrease n_m , seems improbable, as was discussed above. Very low water-contents in these specimens may be responsible, since additive molecular H₂O has a very pronounced effect on indices of refraction (*cf.*, Schreyer & Yoder 1964, Černý & Hawthorne 1976).

OPTICAL ANOMALIES

The most frequent form of optical anomaly in milarite is sector zoning, described by many authors during the last hundred years (*cf.*, Introduction). It consists of growth pyramids underlying each crystal face, with a common apex in the central parts of the crystal. The basal sectors are uniaxial or finely cross-hatched, and the pyramidal and prismatic sectors are biaxial. Other types of anomalies, such as

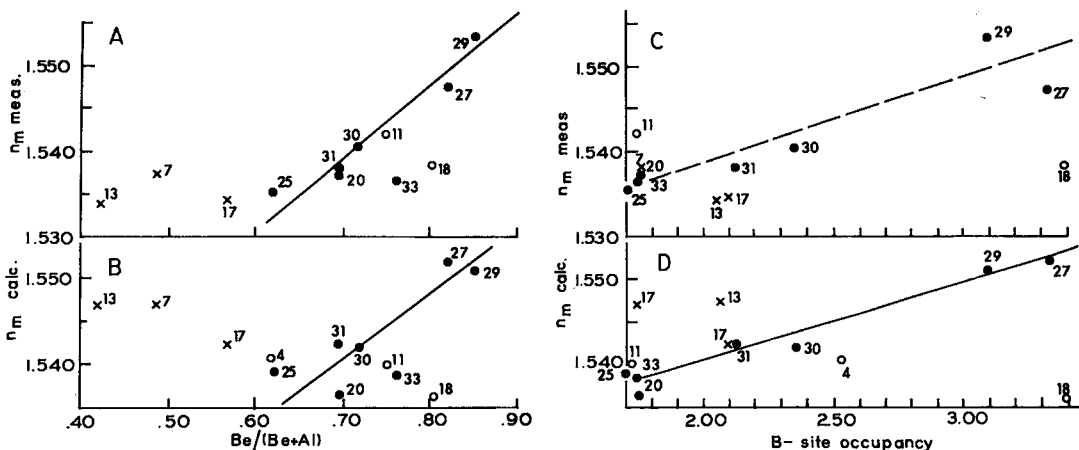


FIG. 10. Index of refraction n_m of milarite: measured values (A and C) and calculated using d_{calc} (B and D) plotted against the Be/(Be + Al) ratio (A and B) and against the B -site occupancy (C and D). Symbols as in Figure 6.

patches of undulatory extinction or micropertite-like moiré patterns with ill-defined sector boundaries, are also known but are much less common.

The optical sectors undergo considerable change upon heating, commonly disappearing completely. Most of the dehydrated "metamilarites" of Rinne (1927) and other authors are optically homogeneous and uniaxial, in agreement with the morphological and structural symmetry. This suggests that the optical anomalies are low-temperature phenomena, caused by ordering or strain during cooling, despite the pyramidal growth-surfaces controlling the sector boundaries.

Three observations argue against ordering as the cause of the optical anomalies. Tetrahedral ordering schemes that would necessarily decrease the symmetry can be developed only for the stoichiometric members of the series; the nonstoichiometric compositions of most natural milarites would prevent long-range order. This is supported by the existing structure refinements from this study and the previous work of Bakakin & Solovyeva (1966) and Bakakin *et al.* (1974), which have not detected any significant deviation from hexagonal symmetry. Also, infrared-absorption spectra obtained for the uniaxial Věžná milarites during this study do not differ in the range of the tetrahedral-cation-oxygen vibrations from those published in the literature for the optically anomalous samples.

Foord & Mills (1978) have reviewed the factors that can cause strain in crystals. Of these, deformation can be ruled out, as most milarites grow freely into open cavities. Temperature or pressure quenches can hardly be responsible, considering the wide variety of low-temperature hydrothermal environments in which milarite originates and the lack of quench effects in the associated minerals. Growth defects have not been studied in milarite, but even if present they could hardly be so widespread and uniform in their effects on the optics as would be required by the abundant occurrence of the anomalies. Sectorial chemical substitutions, however, are well established in milarite. Rinne (1927) noticed that the milky discoloration of water-clear milarite induced by heating and dehydration is initially confined to some optical sectors. Partial analyses of differently colored prismatic and basal growth sectors from the Central Kazakhstan milarite have shown substantial differences in the alkali contents, suggesting different Be/(Be + Al) ratios and water contents (Chistyakova *et al.* 1964).

Compositional sector-zoning with respect to H₂O is particularly interesting, as the water content of the B sites exerts a significant influence on the unit-cell dimensions, counteracting the effect of the Be \rightleftharpoons Al substitution. Dimensional misfit may be expected along boundaries of sectors with different H₂O contents, resulting in strain and optical anomalies that are enhanced during cooling and differential thermal contraction. Thus, the explanation of the optical anomalies proposed by Černý (1960) still holds, in principle, although it was originally based on false premises deduced in part from the structure model of Ito *et al.* (1952) with misplaced water molecules.

Natural milarites with uniaxial optics seem to be confined to the compositions with high alkali, Be and H₂O contents. With continued investigation of milarite from new localities, this may prove to be accidental. At present, it seems that the uniaxial optics are confined not only to a particular compositional range but also to radiating and felty masses of fibrous crystals, suggesting fast nucleation and growth rates. Under these conditions, the growth of compositionally different sectors is unlikely.

CONCLUSIONS

The principal results of the present study, condensed in the abstract, represent a substantial advance in the understanding of milarite. They answer most of the questions raised by apparently inconsistent, erratic variations in composition, and they establish some of the relationships between chemistry and physical properties. Nevertheless, some of the interpretations have had to be made on rather meagre, poor-quality evidence, restricted mainly by scarcity and heterogeneity of material and by the ensuing chemical analytical problems. Further study of milarite from new localities, using advanced analytical techniques on isolated optical-sector units of crystals, is highly desirable.

ACKNOWLEDGEMENTS

The authors are indebted to Dr. T. Hügi (Bern Univ.), Drs. R.I. Gait and J. Mandarino (Royal Ontario Museum, Toronto), Dr. O. von Knorring (University of Leeds), Mr. R. Kristiansen (Torp, Norway), Drs. J.S. White, Jr. (National Museum of Natural History, Washington) and C. Tennyson (T.H., Berlin) for specimens of milarite made available for this study. Dr. J.S. White, Jr. also provided us

with a chemical analysis of milarite from Rössing, and Dr. A.G. Plant (Geological Survey of Canada, Ottawa) kindly performed electron-microprobe analyses of four specimens. X-ray intensity data were collected with the cooperation of the Materials Research Institute, McMaster University, Hamilton, Ontario. Discussions with Drs. W.H. Bauer (University of Illinois, Chicago), M. Fleischer (U.S. Geological Survey, Reston), T. Hügi and W. Schreyer (Ruhr-Universität, Bochum) and unpublished data provided by Dr. G.R. Rossman (California Institute of Technology, Pasadena) helped to clarify different aspects of this study. Mrs. I. Černý and Dr. A.C. Turnock (University of Manitoba, Winnipeg) were of considerable assistance during the experimental work.

The study was started in 1964 at the Geological Institute, Czechoslovak Academy of Sciences in Prague, and finished at the Department of Earth Sciences, University of Manitoba. It was supported by National Research Council of Canada operating grants to the first author and to Dr. R.B. Ferguson.

REFERENCES

- BAKAKIN, V.V., BALKO, V.P. & SOLOVYEVA, L.P. (1975): Crystal structures of milarite, armenite, and sogdianite. *Sov. Phys. Cryst.* 19, 460-462.
- & SOLOVYEVA, L.P. (1966): The crystallochemical analysis of compounds with beryl and milarite structures. *Acta Cryst.* 21, A 41.
- BELOV, N.V. & TARKHOVA, T.N. (1949): Crystal structure of milarite. *Dokl. Akad. Nauk S.S.S.R.* 69, 365-368 (in Russ.).
- & —— (1951): Crystal structure of milarite. *Trudy. Inst. Krist., Akad. Nauk S.S.S.R.* 6, 83-140 (in Russ.).
- BEUS, A.A. (1960): *Geochemistry of Beryllium and Genetic Types of Beryllium Deposits*. Akad. Nauk S.S.S.R., Moscow (in Russ.).
- BROWN, G.E. & GIBBS, G.V. (1969): Refinement of the crystal structure of osumilite. *Amer. Mineral.* 54, 101-116.
- CERNY, P. (1960): Milarite and wellsite from Věžná. *Prace Brněn. Závadny ČSAV* 32, 1(399), 1-14 (in Czech).
- (1963): Epididymite and milarite – alteration products of beryl from Věžná, Czechoslovakia. *Mineral. Mag.* 33, 450-457.
- (1967): Notes on the mineralogy of some West-Moravian pegmatites. *Čas. pro Mineral. a Geol.* 12, 461-463 (in Czech).
- (1968): Berylliumminerale in Pegmatiten von Věžná und ihre Umwandlungen. *Ber. Dtsch. Ges. Geol. Wiss.* B13, 565-578.
- & HAWTHORNE, F.C. (1976): Refractive indices versus alkali contents in beryl: general limitations and applications to some pegmatitic types. *Can. Mineral.* 14, 491-497.
- CHISTYAKOVA, M.B., OSOLODKINA, G.A. & RAZMANOVA, Z.P. (1964): Milarite from Central Kazakhstan. *Dokl. Akad. Nauk S.S.S.R.* 159, 1305-1308 (in Russ.); *Dokl. Acad. Sci. U.S.S.R., Earth Sci. Sect.* 159, 102-105 (1965).
- CROMER, D.T. & LIBERMAN, D. (1970): Relativistic calculation of anomalous scattering factors for X-rays. *J. Chem. Phys.* 53, 1891-1898.
- & MANN, J.B. (1968): X-ray scattering factors computed from numerical Hartree-Fock wave functions. *Acta Cryst.* A24, 321-324.
- DES CLOIZEAUX, A. (1878): Briefliche Mittheilung an Prof. G. vom Rath. *Neues Jahrb. Mineral. Geol. Palaeont.*, 38-46, 370-374.
- FEKLITCHEV, V.G. (1964): *Beryl: Morphology, Composition, and Structure of Crystals*. Nauka, Moscow (in Russ.).
- FINGER, L.W. (1969): RFINE. A Fortran IV computer program for structure factor calculation and least-squares refinement of crystal structures. *Geophys. Lab. Carnegie Inst. Wash.* (unpublished).
- FOORD, E.E. & MILLS, B.A. (1978): Biaxiality in "isometric" and "dimetric" crystals. *Amer. Mineral.* 63, 316-325.
- FORBES, W.C., BAUR, W.H. & KHAN, A.A. (1972): Crystal chemistry of milarite-type minerals. *Amer. Mineral.* 57, 463-472.
- GHOSE, S. & WAN, C. (1978): Zektzerite, NaLiZr Si₆O₁₅: a silicate with six-tetrahedral-repeat double chains. *Amer. Mineral.* 63, 304-310.
- GOLDMAN, D.S. & ROSSMAN, G.R. (1978): The site distribution of iron and anomalous biaxiality in osumilite. *Amer. Mineral.* 63, 490-498.
- GOSSNER, B. & MUSSGNUG, F. (1930): Über Alstonit und Milarit. *Zentralbl. Mineral. (A)*, 220-228.
- GRAESER, S. & HAGER, O. (1961): Über einige neue Fundstellen seltener Mineralien. *Schweiz. Mineral. Petrog. Mitt.* 41, 481-484.
- HAMILTON, W.C. (1965): Significance tests on the crystallographic R-factor. *Acta Cryst.* 18, 502-510.
- HAWTHORNE, F.C. & FERGUSON, R.B. (1975): Refinement of the crystal structure of cryolite. *Can. Mineral.* 13, 377-382.

- HILLEBRAND, W.F., LUNDELL, G.E.F., BRIGHT, H.A. & HOFFMAN, J.I. (1953): *Applied Inorganic Analysis, with Special Reference to the Analysis of Metals, Minerals, and Rocks*. J. Wiley & Sons, New York.
- HÜGI, T. (1956): Verbreitung des Berylliums und der Berylliumminerale in den Schweizer Alpen. *Schweiz. Mineral. Petrog. Mitt.* 36, 497-510.
- & RÖWE, D. (1970): Berylliumminerale und Berylliumgehalte granitischer Gesteine der Alpen. *Schweiz. Mineral. Petrog. Mitt.* 50, 447-480.
- IOVCHEVA, E.I., KUPRIYANOVA, I.I. & SIDORENKO, G.A. (1966): Milarite from Central Asia. *Dokl. Akad. Nauk S.S.S.R.* 170, 1394-1397 (in Russ.); *Dokl. Acad. Sci. U.S.S.R., Earth Sci. Sect.* 170, 160-163 (1967).
- ITO, T., MORIMOTO, N. & SADANAGA, R. (1952): The crystal structure of milarite. *Acta Cryst.* 5, 209-213.
- KENNGOTT, A. (1870): Mitteilungen an Prof. G. Leonhard. *Neues Jahrb. Mineral. Geol. Palaeont.*, 80-81.
- KHAN, A.A., BAUR, W.H. & FORBES, W.C. (1971): Synthetic magnesium merrihueite, dipotassium pentamagnesium dodecasilicate: a tetrahedral magnesian silicate framework crystal structure. *Acta Cryst.* B28, 267-272.
- KUSCHEL, H. (1877): Mitteilung an Prof. G. Leonhard. *Neues Jahrb. Mineral. Geol. Palaeont.*, 925-926.
- LUDWIG, E. (1877): Ueber den Milarit. *Tschermaks Mineral. Mitt.*, 347-352.
- MERLINO, S. (1969): Tuhualite crystal structure. *Science* 166, 1399-1401.
- NOVIKOVA, M.I. (1972): Milarite from Eastern Siberia. *Trudy Mineral. Mus. Akad. Nauk S.S.S.R.* 21, 188-192 (In Russ.).
- OFTEDAL, I. & SÆBØ, P.C. (1965): Contributions to the mineralogy of Norway. 30. Minerals from nordmarkite druses. *Norsk Geol. Tidsskr.* 45, 171-175.
- OLSEN, E. & BUNCH, T.E. (1970): Compositions of natural osmilites. *Amer. Mineral.* 55, 875-879.
- PALACHE, C. (1931): On the presence of beryllium in milarite. *Amer. Mineral.* 16, 469-470.
- PARKER, R.L. (1954): *Die Mineralfunde der Schweizer Alpen*. Wepf & Co. Verlag, Basel, Switzerland.
- PASHEVA, Z.P. & TARKHOVA, T.N. (1953): On the crystal structure of milarite. *Dokl. Akad. Nauk S.S.S.R.* 88, 807-810 (in Russ.).
- PUSHCHAROVSKII, D. YU., BAATARYN, T., POBEDIMSKAYA, E.A. & BELOV, N.V. (1972): The crystal structure of the zinc analog of milarite. *Sov. Phys. Cryst.* 16, 628-630.
- RAADE, G. (1966): A new Norwegian occurrence of milarite. *Norsk Geol. Tidsskr.* 46, 122-123.
- RINNE, F. (1885): Über Milarit, Apophyllit und Rutil. *Neues Jahrb. Mineral. Geol. Palaeont.* 11, 1-24.
- (1927): Milarit und Metamilarit. *Centralbl. Mineral. A*, 1-14.
- RUCKLIDGE, J. & GASPARRINI, E. (1969): Electron microprobe analytical data reduction, *EMPADR VII. Dep. Geol., Univ. Toronto*.
- SCHREYER, W. & YODER, H.S., JR. (1964): The system Mg-cordierite-H₂O and related rocks. *Neues Jahrb. Mineral. Abh.* 101, 271-342.
- SOSEDKO, T.A. (1960): An occurrence of milarite on the Kola Peninsula. *Dokl. Akad. Nauk S.S.S.R.* 131, 643-646 (in Russ.); *Dokl. Acad. Sci. U.S.S.R., Earth Sci. Sect.* 131, 389-392.
- & TELESHEVA, R.L. (1962): Chemical composition of milarite. *Dokl. Akad. Nauk S.S.S.R.* 146, 437-439 (in Russ.); *Dokl. Acad. Sci. U.S.S.R., Earth Sci. Sect.* 146, 112-114 (1964).
- STANĚK, J. (1964): Milarite and triplite from the Marsík pegmatite in northern Moravia. *Acta Mus. Moraviae* 49, 33-38 (in Czech).
- TENNYSON, C. (1960): Berylliumminerale und ihre pegmatitische Paragenese in den Graniten von Tittling/Bayerischer Wald. *Neues Jahrb. Mineral. Abh.* 94, 1253-1265.
- VON KNORRING, O. (1973): Notes on pegmatite minerals from Rwanda, Uganda and South West Africa. *17th Ann. Rep. Res. Inst. Afr. Geol. Univ. Leeds*, 72-73.

Received March 1979, revised manuscript accepted October 1979.